Int. Journal of Refractory Metals and Hard Materials 28 (2010) 692–697

Contents lists available at ScienceDirect

Int. Journal of Refractory Metals and Hard Materials

journal homepage: www.elsevier.com/locate/IJRMHM

High temperature fracture experiments on tungsten–rhenium alloys☆

Stefan Wurster [a,*], Bernd Gludovatz [a,b], Reinhard Pippan [a,b]

[a] Erich Schmid Institute of Materials Science of the Austrian Academy of Sciences, Jahnstraße 12, A-8700 Leoben, Austria
[b] CD Laboratory of Local Analysis of Deformation and Fracture, Jahnstraße 12, A-8700 Leoben, Austria

ARTICLE INFO

Article history:
Received 14 December 2009
Accepted 12 March 2010

Keywords:
Tungsten–rhenium alloys
Recrystallization
Fracture toughness
High temperature fracture experiments

ABSTRACT

A big problem when using tungsten as plasma facing components in a future fusion reactor is the very low fracture toughness at low temperatures. Tungsten–rhenium alloys outclasses other tungsten-based materials in terms of increased ductility. We study the reason for this positive effect by investigating the influence of rhenium on the fracture process of tungsten–rhenium alloys at different temperatures (between room temperature and 900 C). The experiments are performed in a furnace-equipped tensile testing machine with a vacuum chamber, which allows us to perform fracture experiments at elevated temperature without oxidizing the material. Antecedent and subsequent electron backscattered diffraction scans are used to analyse the extent of plastic deformation and the interaction of plastic deformation and the fracture process. Furthermore, the consequences of recrystallization on the fracture process of tungsten–rhenium alloys will be analysed.

1. Introduction

Tungsten materials are considered to be implemented in the International Thermonuclear Experimental Reactor (ITER) in Cadarache, France, and in future fusion reactors as plasma facing materials in the main chamber, other proposed materials are beryllium and carbon fibre composites. Tungsten-based components, either in the shape of bulk or coated parts, will be placed in the divertor region [1]. The first wall, enclosing the plasma, is exposed to challenging conditions: high thermal fluxes up to several MWm^{-2},high operational temperatures and large temperature gradients. Exposure to radiation has to be considered too. Bolt et al. [2] estimate the neutron flux at the first wall of first commercial fusion power reactors after ITER to lead to 150 displacements per atoms (dpa). Beside good mechanical properties at high temperatures, tungsten and tungsten alloys feature high melting points and other superior thermal properties such as good thermal shock resistance and good thermal conductivity. In comparison to low-Z materials like beryllium and carbon, tungsten has a lower erosion rate. A disadvantage of high-Z materials in general is the lower tolerable impurity concentration inside the fusion reactor's plasma; otherwise, the radiation losses of the plasma would be too high. This fact might be outbalanced by the lower sputtering yield of tungsten. Another disadvantage of tungsten in particular is its low fracture toughness, low elongation and small reduction in area at fracture at low temperatures, respectively its high ductile to brittle transition temperature (DBTT), complicating its machinability at room temperature. Nevertheless, the capability of application of tungsten as a plasma facing material has already been proven in the ASDEX (Axially Symmetric Divertor EXperiment) Upgrade tokamak [2].

It has been well known since the sixties and seventies, after intens research programmes related to aircraft and spacecraft technique, that alloying of tungsten with rhenium improves the mechanical behaviour of tungsten, which means lowering of DBTT [3–6]. In the following decades, the information on e.g. fracture behaviour of W–Re alloys is rather sparse [7], which might be related to the fact that Re is a very scarce – its abundance is more likely to be measured in ppt instead of ppm – and thus expensive metal. It is not planned to be used at high concentrations at a large, industrial scale. Nevertheless, not negligible amounts of rhenium and in succession osmium will be produced by transmutation of W due to neutron irradiation [8], implicating the existence of Re within the fusion reactor even when assuming pure W to be the used. However, the development of a strategy to enhance the mechanical behaviour of tungsten alloys is the main reason why the investigation is of interest.

2. Experimental procedure

For fracture toughness experiments, we used an alloy of nominally 26% Re. Closer examination of the as-received material

☆ This publication was presented at the 17th Plansee Seminar in Reutte, Austria, from 25th to 29th May, 2009.

* Corresponding author: S. Wurster, Erich Schmid Institute of Materials Science, Jahnstrasse 12, A-8700 Leoben, Austria. Tel.: +43 (0) 3842 804 325; fax: +43 (0) 3842 804 116.
E-mail address: stefan.wurster@unileoben.ac.at (S. Wurster).

0263-4368/$ – see front matter © 2010 Elsevier Ltd. All rights reserved.
doi:10.1016/j.ijrmhm.2010.03.002

with energy-dispersive X-ray spectroscopy (EDX) determined the rhenium content to be 26.8 wt.% corresponding to 26.5 at.%. The small difference in atom- and weight-percent is related to the close proximity of tungsten (No. 74) and rhenium (No. 75) in the periodic system of elements. No evidence was found that rhenium and tungsten are no solid solution, although the composition of the presented alloy is quite close to the brittle -phase. Out of an as-forged rod with a diameter of 18 mm, compact tension (CT) specimens with thicknesses of B 3 mm and widths W 6 mm were manufactured.

In this study, we compare the fracture behaviour of the as-worked and subsequently stress-relieved W26Re alloy with the recrystallized alloy. After recrystallization of the specimens for 2 h at 2000 C in hydrogen atmosphere, notches (length 3 mm) were produced with a cutting disc in C–R-direction according to ASTM E399-90 [9]. The first letter of this code – used for describing crack geometry in relation to the rod axis – represents the direction normal to the crack plane and the second letter represents the direction of expected crack propagation. Assuming a cylinder, representing the starting material, circumferential (C), longitudinal (L) and radial (R) directions form an orthogonal coordinate system, in which the crack system is positioned. After recrystallization, the previously chosen crack orientation should not have a significant influence on the fracture behaviour due to the more globular shape of the grains and low crystallographic texture. The blunt notches were sharpened by succeeding razor blade polishing technique and cyclic compression [10] up to several 10,000 cycles; the result was a sharp pre-crack penetrating the whole width of the specimen. The influence of recrystallization on the microstructure is visible when checking Fig. 3(a) against Fig. 3(b) and (c). The well recrystallized microstructure is clearly evident from the uniform colour of the grains. Forging induces significant changes crystal orientation in the grains and the formation of a subgrain structure becomes visible in Fig. 3(a).

In addition to the standard microstructural characterization, electron backscatter diffraction scans (EBSD) were made before and after recrystallization of the fracture mechanics samples by use of a Zeiss 1525 scanning electron microscope equipped with an EDAX EBSD system. Evaluation of scans was made with Orientation Imaging Microscopy (OIM) software. Using the support of image quality maps, provided by OIM software, the ends of cyclic-compression-induced cracks are easily allocatable. Scans made after recrystallization and before breaking the specimens can then be compared with scans made after the experiment (Fig. 3(c)). This picture permits to estimate the amount of plastic deformation and the size of the plastically deformed region at different temperatures.

Specimens were tested in atmosphere at room temperature and at 300 C and in a furnace- and vacuum chamber equipped tensile testing machine (Fig. 1) at higher temperatures. The vacuum chamber is capable of reaching pressures of 2 10^{-5} mbar. During the experiments, when reaching temperatures up to about 900 C, the pressure increases but does not exceed 10^{-2} mbar. 1000 C is the as-designed temperature limit of the furnace. Temperature is measured with thermocouples of type K. Force, temperature, time and – owing to a constant crosshead speed – the displacement of the crosshead are recorded. The crosshead speed was set at 0.4 mm min^{-1} for all experiments. An example for recorded load vs. time diagram is shown in Fig. 2, for a specimen tested at 300 C in atmosphere. As it is shown there, the maximal difference in force, representing P_{max}, is taken for evaluation of a conditional K_Q value for fracture toughness according to following equation [9]

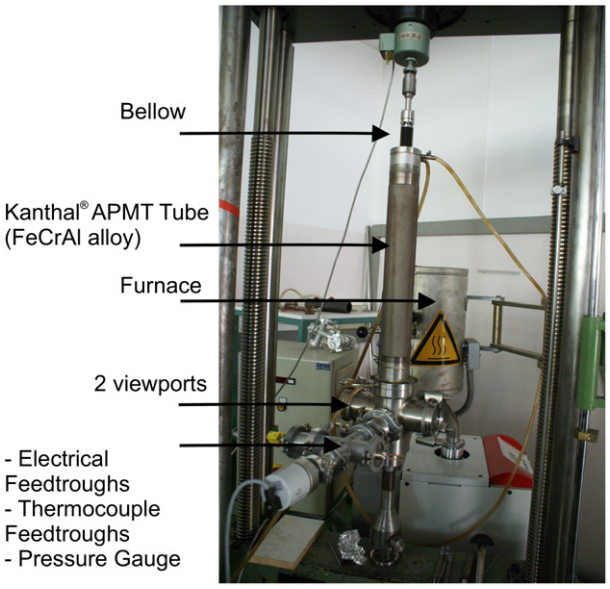

Fig. 1. Assembly of the cylindrical vacuum chamber mounted inside the furnace-equipped tensile testing machine. The device is also equipped with a potential drop method measurement to determine the crack extension during loading.

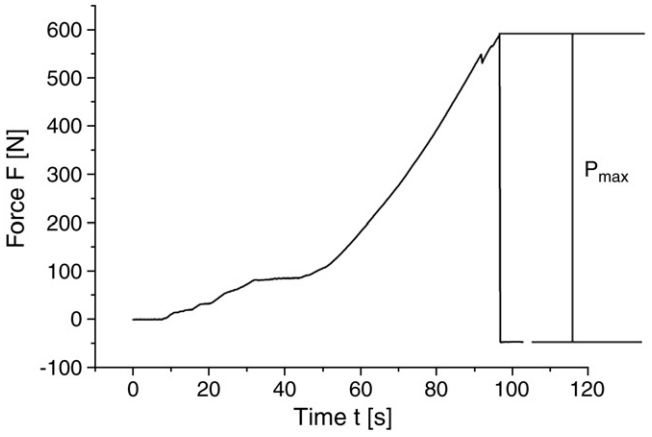

Fig. 2. Load vs. time recording for specimen tested in atmosphere at 300 C, P_{max} is taken for evaluation of K_Q.

$$K_Q = \frac{P_Q}{B * W^{1/2}} * \frac{(2 + \frac{a}{W}) * \left(0.886 + 4.64 * \frac{a}{W} - 13.32 * \frac{a^2}{W^2} + 14.72 * \frac{a^3}{W^3} - 5.6 * \frac{a^4}{W^4}\right)}{(1 - \frac{a}{W})^{3/2}} \quad (1)$$

This test value, K_Q, as well as the experiment itself has to fulfill certain requirements to represent a valid K_{IC} value. The size of the specimen has to fulfill: B and $a > 2.5\ (K_{IC}/_{YS})^2$. $_{YS}$ is the 0.2% offset yield strength of the material for the temperature and loading rate

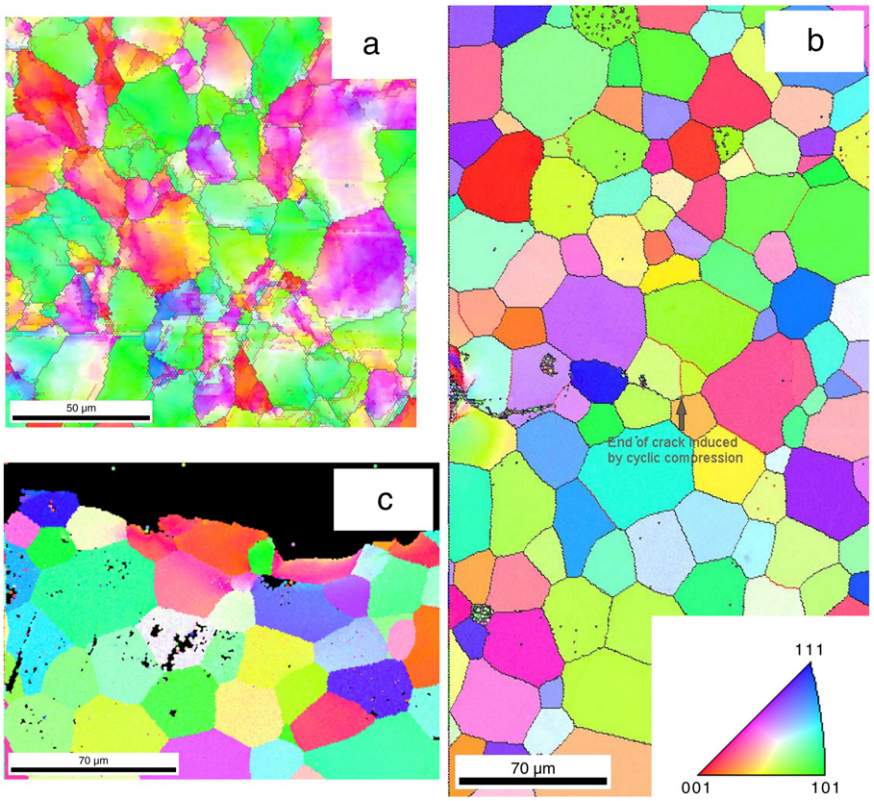

Fig. 3. (a) Inverse Pole Figure (IPF) compiled by an EBSD – scan in longitudinal direction of W26Re alloy in as-worked condition showing a larger amount of misorientation within the grains in comparison to recrystallized material depicted in (b) which shows an IPF of as-recrystallized material (2 h at 2000 C in hydrogen atmosphere). Insert shows the colour code for IPF. (c) IPF of one half of the specimen after breaking at 300 C in atmosphere showing plastically deformed grains close to the crack path. Cleanup of all IPFs were conducted with OIM software.

of the test. The results from these experiments are compared with earlier experiments [11], which were made with the as-forged and stress-relieved tungsten–rhenium alloy, representing the initial condition of the used recrystallized alloy. Three-Point-Bending (3 PB) specimens, sizing 3 6 24 mm^3, were fabricated in L–R-orientation out of the rod. L–R sample geometry can be described as follows: the normal on the crack plane is equivalent to the rod axis and the expected crack propagation direction is along the radius of the rod. Again, the pre-cracks were prepared with the diamond wire saw and razor blade, prior to final fatigue crack initiation under cyclic compression. These 3 PB specimens were tested at room temperature and up to 600 C according to [9]. Heating was carried out by radiation heating and the crosshead speed was 0.03567 mm min^{-1}, about 9% of speed used for testing of recrystallized material.

3. Results and discussion

The results of fracture toughness experiments are summarized in Table 1. The yield strength $_{YS}$ was taken from [3], where the influence of temperature on the yield stress of a W25Re alloy, recrystallized at 2255 K for 1 h, is presented. For higher temperature, yield stresses where linearly extrapolated based on yield stresses for temperatures ranging from 330 to 580 C. With this data it is possible to estimate whether the K_Q values fulfill the above mentioned criterion for being valid K_{IC} values or not. The specimen fractured at 300 C is 30% too small to accommodate the plane strain conditions, for 600 and 870 C, the specimens are too small by one order of magnitude to fulfill this requirements of linear elastic fracture mechanic (LEFM). Regarding the experiments on 3 PB-specimens, the K-values measured at 400 and 600 C are not valid according LEFM. But, all these determined values can be used at least as a lower limit for fracture toughness.

Table 1
Fracture toughness values for four recrystallized W26Re CT-specimens, tested at different temperatures, in atmosphere for room temperature – 300 C, in vacuum for 600–870 C, in comparison with K_Q – values for tungsten–rhenium alloy in as-forged condition, 3 PB – specimens. Those marked with $^{(\uparrow)}$ represent lower limits for fracture toughness. Value of K_Q for liquid nitrogen temperature was taken from Fig. 14 in [12].

Testing temperature (C)	K_Q, recrystallized (MPa $m^{1/2}$)	K_Q, forged (MPa $m^{1/2}$)
−196		38
20	22.8	54.2
300	25.9	–
400	–	65.4 (↑)
600	57.7 (↑)	52.5 (↑)
870	40.5 (↑)	

The bolts, made of lanthanum-doped tungsten, utilized for an experiment at 870 C failed at the maximum load, as the diameter of the bolts, which agreed to ASTM E399-90, is too small. In fact, it was not possible to fracture the specimen in two parts, nevertheless first crack propagation took place. So, the experiment was successful in terms of obtaining a lower limit value for fracture toughness. This resulting fracture toughness is regarded to be the crack initiation fracture toughness. Scanning electron micrographs taken in alignment of the propagated crack were taken (Fig. 4(e) and (f)). Appearing maximum load was used for evaluating a preliminary fracture toughness value. Due to this behaviour, a 3 PB-bending apparatus capable of working in vacuum at high temperatures is going to be constructed.

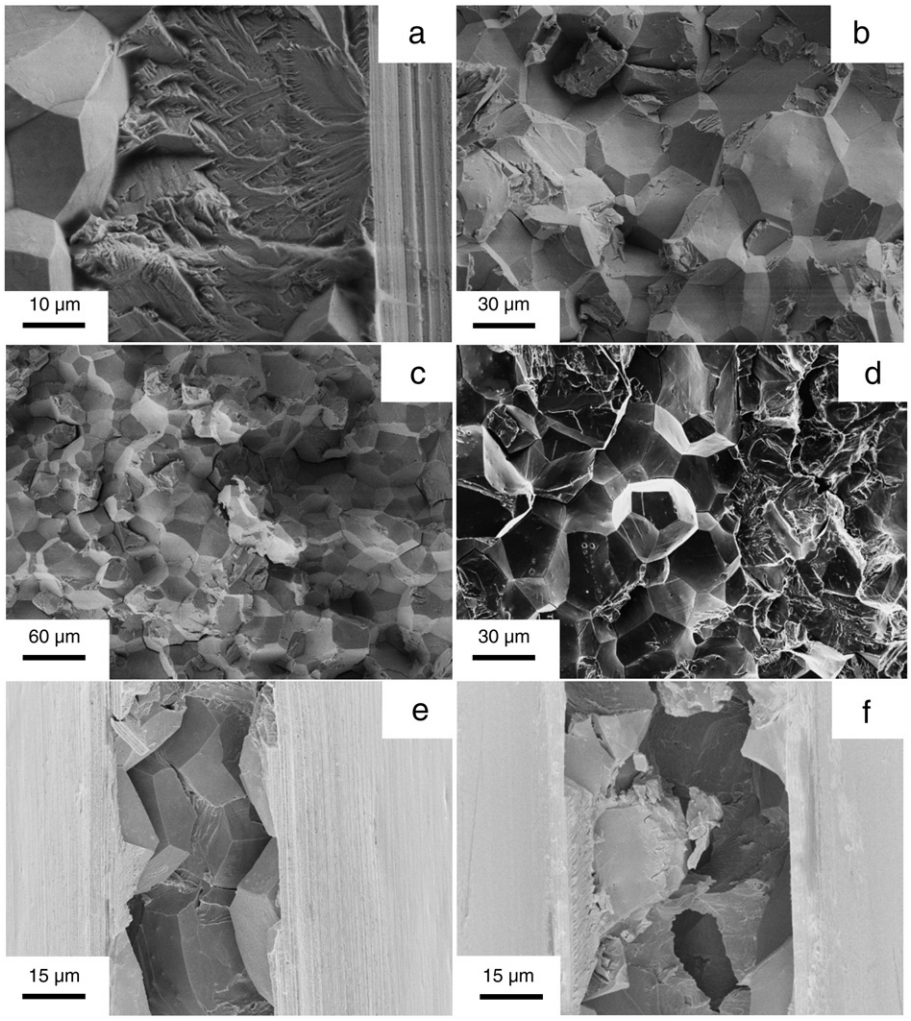

Fig. 4. (a) crack induced by cyclic compression; (b), (c) and (d) fracture surfaces of specimens tested at room temperature, 300 C and 600 C showing an increasing part of transcrystalline fracture for 600 C; (e) and (f) scanning electron micrographs taken of the opened up notch of the specimen tested at 870 C, showing again both transcrystalline and intercrystalline fracture.

The fracture toughness of the as-forged material does not show an isotropic behaviour, as it is lowered by about more than a factor of 2, from 38 MPa $m^{1/2}$ to 17 MPa $m^{1/2}$ [12], when changing the sample geometry from L–R to C–R. In case of C–R sample geometry, the crack front does not propagate perpendicular to the elongated grain structure but these elongated grains are now parallel to the crack front. As the recrystallized samples were tested in C–R sample geometry too, it should be stated that the decrease of fracture toughness is not because of a changed testing direction, as the aspect ratio of the recrystallized grains is much closer to one.

EBSD scans were made before and after breaking the specimens and it is possible to recognize grains in both Inverse Pole Figures (IPF). For instance, the blue grain in the centre of Fig. 3(b) is also identifiable on picture (c) at top left, which was made after fracturing. Slight changes of basic colouring of grains originate from a somewhat changed angle of fitting of the specimen. These IPFs can reveal the plastic deformation of grains, respectively orientation changes inside a grain near the crack path. Scans made for samples tested at room temperature show plastic deformation just very close to the crack path. When fracturing at 300 C, (Fig. 3(c)) more grains experience plastic deformation, also those which are one grain diameter away from the crack path are affected. The size of the plastically deformed areas and the amount of misorientation increases when experiments are conducted at higher temperatures. Measuring the crystallographic orientation within one grain makes it possible to compare the amount of plastic deformation at different temperatures and for different tungsten alloys. When relating the orientation changes in a previously recrystallized grain with the amount of emerging dislocation, the combination of dislocation nucleation and dislocation movement seems to be enhanced the in tungsten–rhenium alloy than in other recrystallized tungsten materials. We plan to treat this topic in a more detailed way in a forthcoming publication.

The fracture surfaces of all recrystallized specimens reveal both intercrystalline and transcrystalline fracture with an increasing tendency towards transcrystalline fracture at elevated temperatures. The fact that specimens broken at room temperature and 300 °C feature almost similar fracture toughness is supported by the fact that they show the same kind of fracture – mostly along the grain boundaries. Fracture toughness for specimens tested at elevated temperatures is higher, which is reflected in the larger amount of transcrystalline fracture. Therefore, the amount of transcrystalline fracture seems to be correlated to the fracture toughness of the samples. Specimens made of the as-forged material show a by far larger extent of transcrystalline fracture (Fig. 5) even at room temperature with a larger plastic deformation of

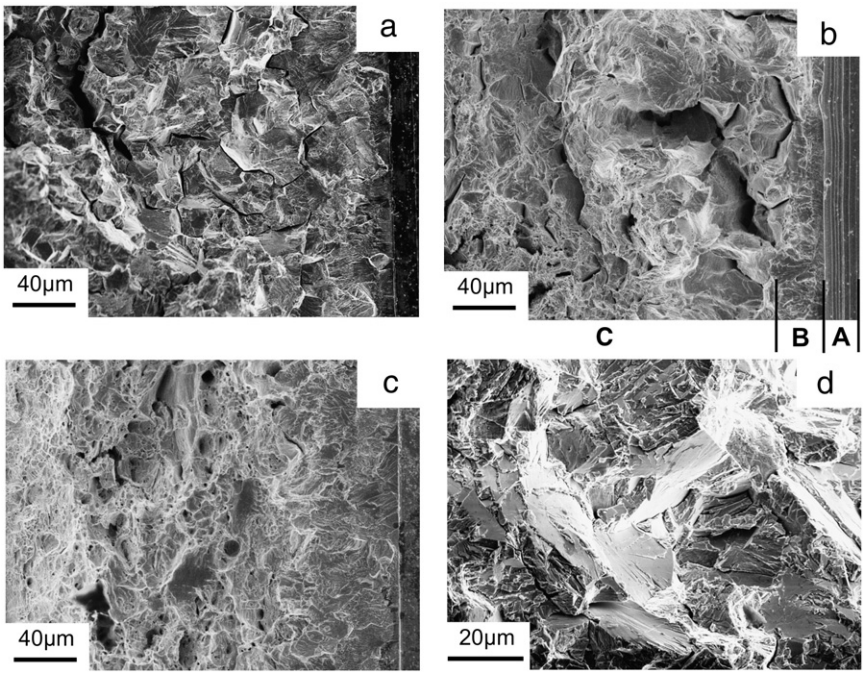

Fig. 5. Scanning electron micrographs of 3 PB specimens broken at (a) room temperature, (b) 400 C, (c) 600 C, (d) −196 C. Intersections in (b) show pre-crack made by razor blade sharpening (A), fatigue crack induced by cyclic compression (B) as well as the fracture surface (C).

grain boundaries compared to recrystallized material. Fracture toughness is about twice as high.

4. Conclusion

Alloying tungsten with rhenium leads to an increase of fracture toughness of tungsten. In our case, this was verified for a W26Re alloy in both stress-relieved as-worked and recrystallized condition. Recrystallization, which might happen at high temperatures plasma facing materials are exposed to in a fusion reactor, changes the picture and lowers the fracture toughness again. In case of the recrystallized W26Re alloy, the fracture toughness was lowered by approximately 50% when taking at hand the samples, which were tested at room temperature and 300 C. Nevertheless, this recrystallized material outclasses pure recrystallized tungsten by about a factor of 3. Inverse pole figures from EBSD scans reveal a higher crystal orientation gradient in the tungsten–rhenium alloy. Considering semi-brittle fracture, dislocations are emitted from the crack tip as the stress intensity is increased and before crack propagation takes place. These dislocations, are the reason for the tilting of the crystals close to the crack flanks in respect to the recrystallized grain, which shows the same crystallographic orientation everywhere. As the tilting of the alloyed material is higher, more dislocations have to be generated in tungsten–rhenium than in tungsten. For an increase in dislocation nucleation, the mobility of screw dislocation is of importance. Our group [13] has shown with simulations basing on density functional theory that alloying tungsten with rhenium leads to a decrease in Peierls stress for the screw dislocations and hence to an increased mobility of dislocations. With increasing testing temperature, dislocation sources in grains at a certain distance from the crack flanks get activated and these grains experience plastic deformation too.

In addition, there is a marked difference of fracture morphology between the as-worked and the recrystallized tungsten–rhenium alloy. Scanning electron micrographs identify the grain boundaries of the recrystallized material to be the weakest link. Reasons for this behaviour are numerous. Impurities like oxygen, phosphorous, fluor or sulfur, which might be uniformly dispersed in the as-worked material, may perhaps get accumulated during the recrystallization process at the moving grain boundaries. Furthermore, the marked difference in dislocation density, texture and subgrain structure may influence the fracture behaviour to a certain extent. Within the context of this work, it is not possible to conclude to what level the above mentioned parameters effect the fracture behaviour of these materials. More work will be carried out on these topics, especially regarding the impurities in tungsten alloys.

Disclaimer

This work, supported by the European Communities under the Contract of Association between EURATOM and the Austrian Academy of Sciences, was carried out within the framework of the European Fusion Development Agreement. The views and opinions expressed herein do not necessarily reflect those of the European Commission.

References

[1] Hirai T, Maier H, Rubel M, Mertens P, Neu R, Gauthier E, et al. JET EFDA Contributors. R&D on full tungsten divertor and beryllium wall for JET IER-like wall project. Fusion Eng Des 2007;182:1839–45.
[2] Bolt H, Barabash V, Krauss W, Linke J, Neu R, Suzuki S, et al. ASDEX Upgrade Team. Materials for the plasma-facing components of fusion reactors. J Nucl Mater 2004;329–333:66–73.
[3] Raffo P. Yielding and fracture in tungsten and tungsten–rhenium alloys. J Less Common Metal 1969;17:133–49.
[4] Geach GA, Hughes JE. The alloys of rhenium with molybdenum or with tungsten and having good high temperature properties. In: Proc 2nd International Plansee Seminar; 1955. p. 245–53.
[5] Klopp WD, Witzke WR, Raffo PL. Mechanical properties of dilute tungsten–rhenium alloys. NASA Technical Note NASA TN D-3483, Washington, DC; 1966.
[6] Jaffee RI, Sims CT, Harwood JJ. The effect of rhenium on the fabricability and ductility of molybdenum and tungsten. In: Proc 3rd International Plansee Seminar; 1958. p. 380–411.
[7] Mutoh Y, Ichikawa K, Nagata K, Takeuchi M. Effect of rhenium addition on fracture toughness of tungsten at elevated temperatures. J Mater Sci 1995;30:770–5.

[8] Noda T, Fijita M. Effect of neutron spectra on the transmutation of first wall elements. J Nucl Mater 1996;233–237:1491–5.
[9] Annual Book of ASTM Standards. Metal test methods and analytical procedures, vol. 03.01; 1993; p. 509–39.
[10] Pippan R. The growth of short cracks under cyclic compression. Fatigue Fract Eng Mater Struct 1987;9:319–28.
[11] Kiener D, Kreuzer H, Pippan R. Report for TASK of the EFDA Programme TW4-TTMA-002 "Tungsten Alloys Development"; 2004.
[12] Kreuzer H, Faleschini M, Gludovatz B. Report for TASK of the EFDA Programme TW5-TTMA-002 "Tungsten Alloy Development"; 2006.
[13] Romaner L, Ambrosch-Draxl C, Pippan R. Effect of Rhenium on the Dislocation Core Structure in Tungsten. Phys Rev Lett 2010;104(19):195503.